






## Article

# TRPC6-Mediated $\text{Zn}^{2+}$ Influx Negatively Regulates Contractile Differentiation of Vascular Smooth Muscle Cells

Chenlin Su <sup>1,†</sup>, Xinya Mi <sup>1,†</sup> , Tomoya Ito <sup>1</sup> , Yuri Kato <sup>1</sup> , Akiyuki Nishimura <sup>2,3,4</sup> , Ryu Nagata <sup>5</sup>, Yasuo Mori <sup>6</sup> and Motohiro Nishida <sup>1,2,3,4,\*</sup> 

<sup>1</sup> Graduate School of Pharmaceutical Sciences, Kyushu University, Fukuoka 812-8582, Japan; yu-kato@phar.kyushu-u.ac.jp (Y.K.)

<sup>2</sup> National Institute for Physiological Science (NIPS), National Institutes of Natural Sciences, Okazaki 444-8787, Japan

<sup>3</sup> Exploratory Research Center on Life and Living Systems (ExCELLS), National Institutes of Natural Science, Okazaki 444-8787, Japan

<sup>4</sup> Department of Physiological Sciences, SOKENDAI (School of Life Science, The Graduate University for Advanced Studies), Okazaki 444-8787, Japan

<sup>5</sup> Graduate School of Pharmaceutical Sciences, Osaka University, Osaka 565-0871, Japan

<sup>6</sup> Graduate School of Engineering, Kyoto University, Kyoto 615-8510, Japan

\* Correspondence: nishida@phar.kyushu-u.ac.jp; Tel.: +81-92-642-6556

† These authors contributed equally to this work.

**Abstract:** Vascular smooth muscle cells (VSMCs) can dynamically change their phenotype between contractile and synthetic forms in response to environmental stress, which is pivotal in maintaining vascular homeostasis and mediating pathological remodeling of blood vessels. We previously reported that suppression of canonical transient receptor potential 6 (TRPC6) channel-mediated cation entry sustains VSMCs contractile phenotype and promotes the blood flow recovery after hindlimb ischemia in mice. We also reported that  $\text{Zn}^{2+}$ , a metal biomolecule mobilized by TRPC6 channel activation, exerts potential beneficial effects on cardiac contractility and remodeling. Therefore, we hypothesized that TRPC6-mediated  $\text{Zn}^{2+}$  influx participates in phenotype switching of VSMCs and vascular remodeling. We established rat aortic smooth muscle cells (RAoSMCs) stably expressing wild type (WT) and  $\text{Zn}^{2+}$  only impermeable TRPC6 (KYD) mutant. Although the resting phenotypes were similar in both RAoSMCs, pharmacological TRPC6 activation by PP2Z prevented the transforming growth factor (TGF)  $\beta$ -induced reduction in the intracellular  $\text{Zn}^{2+}$  amount and contractile differentiation in RAoSMCs (WT), but failed to prevent them in RAoSMCs (KYD). There were no significant differences in TRPC6-dependent cation currents among all RAoSMCs pretreated with or without TGF $\beta$  and/or PP2Z, suggesting that TRPC6 channels are functionally expressed in RAoSMCs regardless of their phenotype. Treatment of mice with PP2Z attenuated the progression of vascular remodeling caused by chronic angiotensin II infusion. These results suggest that  $\text{Zn}^{2+}$  influx through TRPC6 channels negatively regulates the TGF $\beta$ -induced contractile differentiation of VSMCs and the progression of vascular remodeling in rodents.

**Keywords:**  $\text{Zn}^{2+}$  influx; TRPC6 channel; phenotypic switching; vascular smooth muscle cells



Academic Editors: Eun-Woo Lee and Hye Jin Kang

Received: 27 December 2024

Revised: 5 February 2025

Accepted: 10 February 2025

Published: 12 February 2025

**Citation:** Su, C.; Mi, X.; Ito, T.; Kato, Y.; Nishimura, A.; Nagata, R.; Mori, Y.; Nishida, M. TRPC6-Mediated  $\text{Zn}^{2+}$  Influx Negatively Regulates Contractile Differentiation of Vascular Smooth Muscle Cells.

*Biomolecules* **2025**, *15*, 267. <https://doi.org/10.3390/biom15020267>

**Copyright:** © 2025 by the authors.

Licensee MDPI, Basel, Switzerland.

This article is an open access article

distributed under the terms and

conditions of the Creative Commons

Attribution (CC BY) license

(<https://creativecommons.org/licenses/by/4.0/>).

## 1. Introduction

Mature arterial reconfiguration refers to structural and functional changes in the vessel wall that occur in response to pathological conditions, injury, or aging process [1,2]. Vascular smooth muscle cells (VSMCs), the major cell type located in the middle layer of

the arterial vessel wall, contribute to the maintenance of vascular tone and structural stability by alternating with elastic fibers [3–5]. VSMCs exhibit significant plasticity, which allows for dynamic transitions between highly proliferative (synthetic) and fully differentiated (contractile) phenotypes, thereby ensuring vascular maturation [6]. Healthy mature VSMCs exhibit a limited synthetic ability [7], while in response to the pathogenesis of various human cardiovascular diseases, the contractile phenotype is converted into a dedifferentiated synthetic phenotype [8]. For example, in the pathological state of atherosclerosis, changes in the contractile phenotype of VSMCs lead to the narrowing of the vessel diameter and vascular stiffness [5,9–14]. On the other hand, with increased blood volume, vascular tone increases, which causes VSMCs to excessively transition to the contractile phenotype, resulting in chronic hypertension accompanied by a thickening of the medial layer [15]. Therefore, maintaining the ability of VSMCs to switch phenotypes is critical for sustaining vascular homeostasis.

Canonical subfamily members of transient receptor potential (TRPC) proteins form phospholipase C-linked receptor-operated  $\text{Ca}^{2+}$ -permeable non-selective cation channels in vertebrates [16]. Among the TRPC1-TRPC7 subfamily, the pathophysiological roles of TRPC6 have been well investigated in VSMCs [17]. In cultured pulmonary arterial smooth muscle cells (PASMCs), TRPC6 expression is up-regulated after treatment with platelet-derived growth factor through the increase in store-operated  $\text{Ca}^{2+}$  entry, which contributes to hyperplasia by facilitating phenotype switching of PASMCs from contractile to synthetic [18,19]. We have reported that the increased TRPC6 channel activity negatively regulates the promotion of vessel maturation after hindlimb ischemia, potentially contributing to peripheral arterial disease [20]. Suppression of  $\text{Ca}^{2+}$  entry through the TRPC6 channel activated by ischemic stress could make it more switchable to contractile phenotype by reducing the interaction between TRPC6 and phosphatase and tensin homolog deleted on chromosome 10 (PTEN) [21]. However, TRPC6 does not only permeate  $\text{Ca}^{2+}$ ,  $\text{Na}^{+}$  and  $\text{K}^{+}$ , but it also permeates other metal ions, such as  $\text{Zn}^{2+}$  and  $\text{Fe}^{2+}$ . Of note, these characteristics are not conserved in most TRPC6-related TRPC3 and TRPC7 channels [22–26].

$\text{Zn}^{2+}$  permeates from extracellular (approximately 10 nM) into the cells through transporters and ion channels, and most  $\text{Zn}^{2+}$  is believed to be tightly bound to intracellular organelles, for instance, enzymes and metallothioneins [27,28]. While  $\text{Zn}^{2+}$  binds with protein in a labile form, mobile intracellular  $\text{Zn}^{2+}$ , approximately 100 pM, remains to function as a second messenger [27,29]. The pooled  $\text{Zn}^{2+}$  and mobile  $\text{Zn}^{2+}$  provide a different view of the physiological significance of  $\text{Zn}^{2+}$ -binding protein interactions. The critical functions of cellular  $\text{Zn}^{2+}$  signaling underscore potential molecular pathways linking  $\text{Zn}^{2+}$  metabolism to disease progression [30]. The importance of  $\text{Zn}^{2+}$ -permeable ion channels, especially in intracellular  $\text{Zn}^{2+}$  dynamics and  $\text{Zn}^{2+}$ -mediated physiological and pathophysiological processes, is widely recognized [31]. Cellular  $\text{Zn}^{2+}$  capability can be estimated by the treatment with 2,2'-dithiodipyridine (DTDP), which oxidizes  $\text{Zn}^{2+}$ -binding proteins and induces  $\text{Zn}^{2+}$  release from the intracellular  $\text{Zn}^{2+}$  pool [32].  $\text{Zn}^{2+}$  participates in cell proliferation activity through several pathways [33]. For instance,  $\text{Zn}^{2+}$  is essential for insulin-like growth factor-I-induced cell proliferation [34] and nerve growth factor-induced differentiation [35].

Since several reports suggest the beneficial effects of  $\text{Zn}^{2+}$  in the cardiovascular system, we hypothesized that the  $\text{Zn}^{2+}$  influx mediated through the TRPC6 channel may contribute to the maintenance of vascular homeostasis by regulating VSMCs phenotype switching. To investigate the role of TRPC6-mediated  $\text{Zn}^{2+}$  influx in VSMCs phenotype switching, we established rat aortic smooth muscle cells (RAoSMCs) stably expressing TRPC6 wild-type (WT) and TRPC6  $\text{Zn}^{2+}$ -only impermeable mutant (KYD) [25]. We investigated whether pharmacological TRPC6 activation negatively regulates contractile dif-

ferentiation of RAoSMCs by transforming growth factor (TGF)  $\beta$  stimulation. We also investigated whether pharmacological TRPC6 activation has a beneficial effect on vascular remodeling in angiotensin (Ang) II-infused mice.

## 2. Materials and Methods

### 2.1. Animals

All protocols using mice were reviewed and approved by the Animal Care and Use Committee at Kyushu University and performed according to Institutional Guidelines Concerning the Care and Handling of Experimental Animals (approval no. A24-167-1, A24-252-1).

We obtained 129/Sv male mice from the Comparative Medicine Branch, National Institute of Environmental Health Sciences (Research Triangle Park, NC, USA). All mice were group housed in individually ventilated cages (three or four animals per cage) with aspen wood chip bedding and kept under controlled environmental conditions (specific-pathogen-free area, 12 h light/dark cycle, room temperature 21–23 °C, and humidity 50–60%) with free access to standard laboratory food pellets (CLEA Rodent Diet CE-2, CLEA Japan, Tokyo, Japan) and water.

### 2.2. Vascular Remodeling Mice Model

Vascular remodeling was caused by continuous administration of Ang II (PEPTIDE, Cat# 4001, Osaka, Japan). A micro-osmotic pump (Alzet, Cat# 1002, Tokyo, Japan) filled with Ang II (2 mg/kg/day) with or without 2-[4-(2,3-dimethylphenyl)-piperazin-1-yl]-N-(2-ethoxyphenyl) acetamide (PPZ2, 2.5 mg/kg/day) [36], a TRPC3/6/7 channel activator, was embedded intraperitoneally into 129/Sv male mice (8–9 weeks old) for 14 consecutive days. Control mice were administered with the normal saline (NS). The pharmacological efficacy of Ang II was determined by the increase in blood pressure. Blood pressure was measured from the tail using a non-invasive tail-cuff system (Softron, Tokyo, Japan) while the mice were dressed in a special restraint suit and warmed with a heat mat (38 °C).

### 2.3. Immunocytochemistry

Thawed RAoSMCs were used for experiments after at least 5 passages, with almost all RAoSMCs showing a synthetic form, and discarded after 10 passages. RAoSMCs were cultured in culture medium (Dulbecco's modified Eagle's medium (DMEM, low glucose, Thermo Fisher Scientific, MA, USA) supplemented with 10% FBS, 1% penicillin and streptomycin and 2  $\mu$ g/mL Puromycin) at 37 °C in a humidified atmosphere (5% CO<sub>2</sub>, 95% air) [25]. TRPC6 (WT)- and TRPC6 (KYD)-expressing RAoSMCs were established by using retrovirus, and positive cells were selected with puromycin [25]. TRPC6 (WT)- and TRPC6 (KYD)-expressing RAoSMCs were seeded at  $3 \times 10^3$  cells/200  $\mu$ L on 4-well glass-bottom dishes. The cells were treated with 0.1% DMSO, 3  $\mu$ M of PPZ2, 10 ng/mL of TGF $\beta$  with or without PPZ2 in 10  $\mu$ M ZnCl<sub>2</sub> supplied culture medium for 24 h, and then fixed with 4% paraformaldehyde in PBS (Fujifilm Wako, Cat# 045-29795, Osaka, Japan) for 15 min. After washing with PBS for 10 min three times, cells were blocked with blocking-permeabilization solution containing 0.2% Triton X-100 and 10% FBS in PBS for 1 h at room temperature. Cells were overnight incubated with the primary antibodies at 4 °C: anti- $\alpha$ -smooth muscle actin ( $\alpha$ -SMA) (1:500 dilution; eBioscience, Cat# 14-9760-82, CA, USA), anti-smooth muscle 22  $\alpha$  (SM22 $\alpha$ ) (1:500 dilution; Abcam, Cat# 14106, Cambridge, UK) and anti-TRPC6 (1:300 dilution; Thermo Fisher Scientific, Cat# ACC-120, MA, USA). Alexa Fluor 488-conjugated anti-mouse IgG or 488-conjugated anti-rabbit IgG (1:500 dilution; Thermo Fisher Scientific, Cat# A11029 or Cat# A11034, MA, USA) secondary antibodies were applied for 2 h at room temperature in blocking-permeabilization solution.

The nuclei were stained with 4'-6'-diamidino-2-phenylindole (DAPI, 1:10,000 dilution; DOJINDO, Cat# 340-7971, Kumamoto, Japan). The fluorescence images were acquired using a fluorescence microscope (BZ-X800; Keyence, Osaka, Japan) or a confocal microscope (LSM 900; ZEISS, Oberkochen, Germany), and the mean fluorescence intensity/pixel of each cell was analyzed with ImageJ2 (Version: 2.14.0/1.54f) software (National Institutes of Health, Bethesda, MD, USA).

#### 2.4. Cell Proliferation Assay

Cell proliferation was assessed using a Cell Counting Kit (CCK)-8 (DOJINDO, Cat# 347-07621, Kumamoto, Japan). TRPC6 (WT)- and TRPC6 (KYD)-expressing RAoSMCs were seeded at  $5 \times 10^3$  cells in 100  $\mu$ L each well on a 96-well plate. One day after plating, cells were treated with 0.1% DMSO or 3  $\mu$ M of PPZ2 in 10  $\mu$ M ZnCl<sub>2</sub> supplied culture medium for 1 h. Subsequently, each group was co-treated with or without 10 ng/mL of TGF $\beta$  for 24 h. The value of wells with 0.1% DMSO was normalized as a control.

#### 2.5. RAoSMCs Transfection

RAoSMCs were cultured in Dulbecco's modified Eagle's medium (DMEM, low glucose) supplemented with 10% FBS, 1% penicillin and streptomycin at 37 °C in a humidified atmosphere (5% CO<sub>2</sub>, 95% air). A fraction of RAoSMCs were plated in 35 mm culture dishes and transfected with plasmid DNAs (TRPC6 (WT) and TRPC6 (KYD) mutant) [37] using X-tremeGENE9 (Roche, Basel, Switzerland). One day after plating, cells were treated with 0.1% DMSO or 3  $\mu$ M of PPZ2 in 10  $\mu$ M ZnCl<sub>2</sub> supplied culture medium for 1 h. Subsequently, each group was co-treated with or without 10 ng/mL of TGF $\beta$  for 24 h. Then, cells were reseeded onto glass coverslips (3  $\times$  5 mm<sup>2</sup>) in 35 mm culture dishes for patch clamp.

#### 2.6. Zn<sup>2+</sup> Imaging

For the measurement of Zn<sup>2+</sup> influx, TRPC6 (WT)- and TRPC6 (KYD)-expressing RAoSMCs were reseeded onto coverslips (3  $\times$  5 mm<sup>2</sup>) in a 6-well plate with 2 mL culture medium. One day after plating, cells were treated with 0.1% DMSO or 3  $\mu$ M of PPZ2 in 10  $\mu$ M ZnCl<sub>2</sub> supplied culture medium for 1 h. Subsequently, each group was co-treated with or without 10 ng/mL of TGF $\beta$  for 24 h. Then, cells were washed with 1 $\times$  HBSS (10 $\times$  HBSS, Thermo Fisher Scientific, Cat# 14065-056, MA, USA) and loaded with FluoZin-3 (2  $\mu$ M) (Thermo Fisher Scientific, Cat# F24195, MA, USA) for 30 min at 37 °C [25]. After loading, the dye solution was replaced with 1 $\times$  HBSS. Then, 50  $\mu$ M of DTDP (Sigma, Cat# 2127-03-9, Darmstadt, Germany) was applied 2 min after starting measurement, and then N,N,N',N'-tetrakis (2-pyridylmethyl)ethylenediamine (TPEN, 50  $\mu$ M; Zn<sup>2+</sup> chelator)(DOJINDO, Cat# 340-05411, Kumamoto, Japan) was applied 5 min after adding DTDP. Fluorescence images were recorded every 10 s and analyzed using a video image analysis system (Aquacosmos 2.6, Hamamatsu Photonics, Shizuoka, Japan).

#### 2.7. Whole-Cell Patch-Clamp Techniques

The conventional whole-cell patch-clamp technique was used to record resting membrane potential and ion currents in the voltage-clamp models at room temperature with an EPC-10 patch-clamp amplifier (HEKA, Lambrecht, Germany). Patch electrodes with a resistance of 3–4 M $\Omega$  were made from G-1.5 mm borosilicate glass capillaries (Sutter Instrument, CA, USA). We have preliminarily confirmed using electrophysiological experiments that TRPC6 (KYD) mutant specifically lacks Zn<sup>2+</sup> permeability compared with TRPC6 (WT) in HEK293 cells. In this study, the TRPC6 current [38] was measured by the whole-cell patch-clamp technique on TRPC6 WT and KYD mutant overexpressing RAoSMCs. Before patch-clamp measurement, RAoSMCs were treated with 0.1% DMSO or 3  $\mu$ M of PPZ2 in 10  $\mu$ M ZnCl<sub>2</sub> supplied culture medium for 1 h. Subsequently, each group was co-treated

with or without 10 ng/mL of TGF $\beta$  for 24 h. Cells were allowed to settle in the perfusion chamber in the external solution. TRPC6 was recorded in K<sup>+</sup>-free bathing solution including (in mM): 140 NaCl, 5.4 CsCl, 1 CaCl<sub>2</sub>, 1 MgCl<sub>2</sub>, 0.33 NaH<sub>2</sub>PO<sub>4</sub>, 5 HEPES and 5.5 glucose (pH 7.4, adjusted with NaOH). The pipette solution contained (in mM) 120 CsOH, 120 aspartate, 20 CsCl, 2 MgCl<sub>2</sub>, 5 EGTA, 1.5 CaCl<sub>2</sub>, 10 HEPES and 10 glucose (pH 7.2, adjusted with CsOH). Voltage ramps (−100 to +100 mV) of 250 ms were recorded every 2 s from a holding potential of −60 mV.

## 2.8. Immunohistochemical Analysis of Mouse Aortas

The aortas removed from mice were embedded in an optimal cutting temperature compound (Sakura Finetech, Tokyo, Japan) and frozen in liquid nitrogen. Frozen tissues were sliced at 10  $\mu$ m slices by Leica CM1100 (Leica Biosystems, Nussloch, Germany). Sections were fixed with 4% paraformaldehyde for 15 min, then washed with PBS three times. Blocking of the sections was performed with a blocking–permeabilization solution containing 0.2% Triton X-100 and 10% FBS in PBS for 1 h at room temperature. Sections were stained overnight at 4 °C with primary anti-mouse  $\alpha$ -SMA (1:500 dilution, eBioscience, Cat# 14-9760-82, CA, USA) and anti-mouse CD31 (1:200 dilution, BioLegend, Cat# 102401, CA, USA) antibodies, incubated for 2 h with secondary Alexa Fluor 488-conjugated anti-mouse IgG or Alexa Fluor 568-conjugated anti-rat IgG (1:500 dilution; Thermo Fisher Scientific, Cat# A11077, MA, USA) at room temperature in the blocking–permeabilization solution. The specimens were observed with a fluorescence microscope (BZ-X800; Keyence, Osaka, Japan). For the analysis of  $\alpha$ -SMA and CD31 expression in aortas, fluorescence signal intensity within the region of interest (ROI) being made based on  $\alpha$ -SMA fluorescence images was quantified, which was further normalized and represented as a fold increase from before chronic Ang II administration. ImageJ2 (Version: 2.14.0/1.54f) software (National Institutes of Health, Bethesda, MD, USA) was used for all the image analysis.

## 2.9. Statistical Analysis

All results are presented as the mean  $\pm$  SEM from at least three independent experiments. Statistical analyses were performed using GraphPad Prism 9.0 (GraphPad Software, LaJolla, CA, USA), performing the Normality and Lognormality tests with the Shapiro–Wilk test for small sample sizes ( $N < 50$ ) and the Kolmogorov–Smirnov test for larger sample sizes ( $N \geq 50$ ) [39]. When the test indicated  $p > 0.05$ , the data were considered normally distributed. At the same time, the graphic method Q-Q plot is used for the auxiliary test. When data were from three or more groups, one-way analysis of variance (ANOVA) with Tukey’s post hoc test was used for normally distributed data, and the Kruskal–Wallis test with the Dunn test was used for nonparametric data. Sample sizes were at least 5 animals per group subjected to statistical analysis.  $p$  values  $< 0.05$  were considered statistically significant.

# 3. Results

## 3.1. Pharmacological Activation of TRPC6 Channel Prevents TGF $\beta$ -Induced Differentiation on TRPC6 (WT)-Expressing RAoSMCs

TGF $\beta$  is a key cytokine implicated in vascular remodeling, and it has been shown to drive VSMCs toward differentiation state [40–44]. We first examined if pharmacological activation of the TRPC6 channel negatively regulates the TGF $\beta$ -induced contractile differentiation of RAoSMCs. Activation of TRPC3/6/7 channels by PPZ2 treatment markedly decreased the fluorescence intensities of contractile markers, including  $\alpha$ -SMA (Figure 1a,b) and SM22 $\alpha$  (Figure 1c,d) in TGF $\beta$ -induced RAoSMCs. There were significant TRPC6 fluorescence intensities in TRPC6 (WT)-expressing RAoSMCs, compared with



normal RAoSMCs (Figure 1e,f). The protein expression levels of TRPC6 (WT) were not affected by the treatment with PPZ2 or TGF $\beta$  (Figure 1g,h). As the expression level of TRPC6 in smooth muscle cells is much higher compared with that of TRPC3 and TRPC7 [45], these results suggest that activation of the TRPC6 channel negatively regulates the TGF $\beta$ -induced contractile differentiation of RAoSMCs.

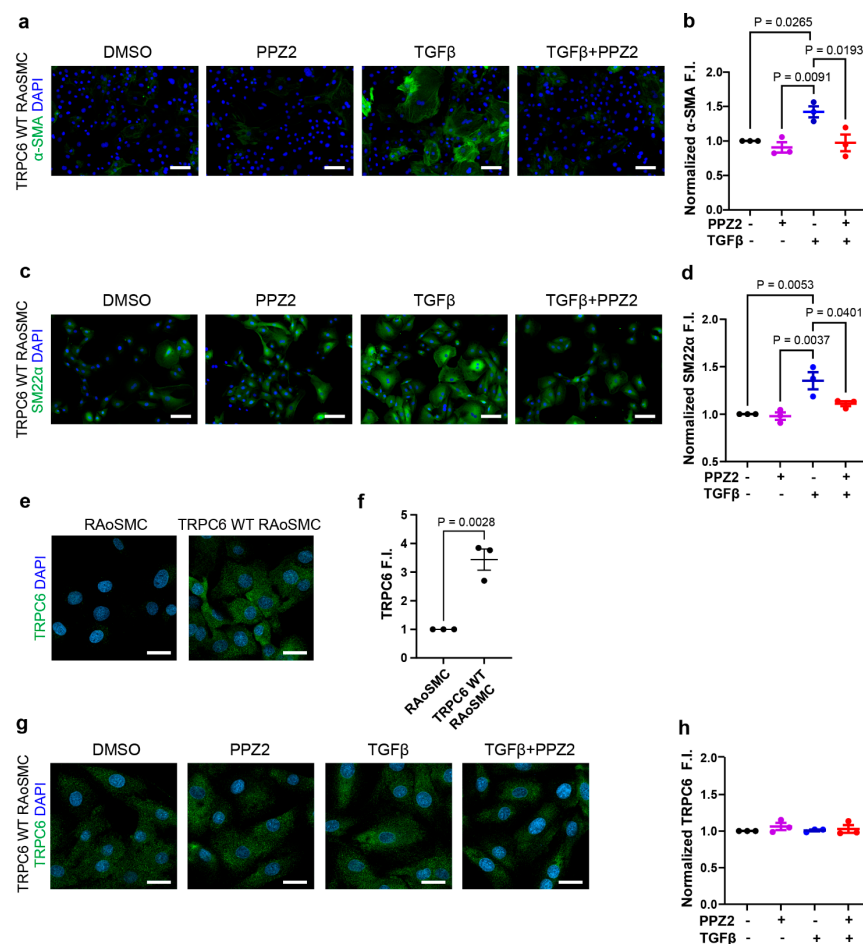


**Figure 1.** Pharmacological activation of TRPC6 prevents the TGF $\beta$ -induced contractile differentiation of TRPC6 (WT)-expressing RAoSMCs: **(a,b)** Representative images and quantification of  $\alpha$ -SMA (green) immunofluorescence intensities in TRPC6 (WT)-expressing RAoSMCs. Scale bars = 50  $\mu$ m. **(c,d)** Representative images and quantification of SM22 $\alpha$  (green) immunofluorescence intensities in TRPC6 (WT)-expressing RAoSMCs. Scale bars = 50  $\mu$ m. **(e,f)** Representative images and quantification of TRPC6 (green) immunofluorescence intensities in RAoSMCs and TRPC6 (WT)-expressing RAoSMCs. Scale bars = 30  $\mu$ m. **(g,h)** Representative images and quantification of TRPC6 (green) immunofluorescence intensities in TRPC6 (WT)-expressing RAoSMCs. Scale bars = 30  $\mu$ m. Nuclei were counterstained with DAPI (blue). Three separate experiments (N = 3) were averaged to produce the data. Data are shown as mean  $\pm$  SEM.  $p < 0.05$  using one-way ANOVA followed by Tukey's post hoc test.

### 3.2. Lacking $Zn^{2+}$ Influx Activity of TRPC6 Fails to Prevent the TGF $\beta$ -Induced Differentiation of RAoSMCs by PPZ2 Treatment

To investigate whether TRPC6-mediated  $Zn^{2+}$  influx contributes to the prevention of TGF $\beta$ -induced VSMCs differentiation by PPZ2, we utilized  $Zn^{2+}$  impermeable TRPC6 mutant (TRPC6 (KYD))-expressing RAoSMCs, as previously reported [25]. The contractile markers of  $\alpha$ -SMA (Figure 2a,b) and SM22 $\alpha$  (Figure 2c,d) fluorescence intensities were similarly increased by TGF $\beta$  stimulation. However, the contractile marker intensity levels under treatment of PPZ2 were not reduced in TGF $\beta$ -stimulated RAoSMCs. The TRPC6 pro-

tein expression levels were also unaffected by treatment with PPZ2 or TGF $\beta$  (Figure 2e,f). The proliferating activities of TRPC6 (WT)- and TRPC6-(KYD)-expressing RAoSMCs were similar even though treated with PPZ2 and/or TGF $\beta$  (Figure 2g,h). These results indicate that TRPC6-mediated Zn<sup>2+</sup> influx activity is critical for the prevention of TGF $\beta$ -induced VSMC differentiation by PPZ2.

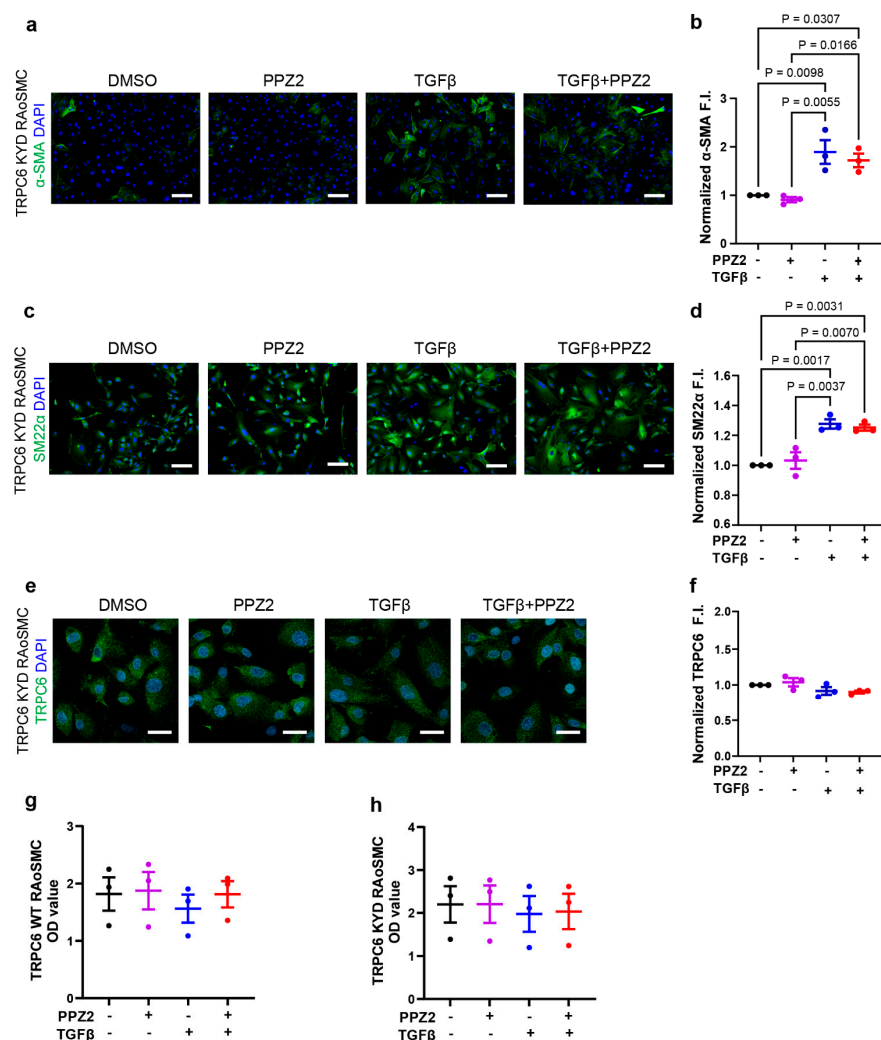


**Figure 2.** Requirement of TRPC6-mediated Zn<sup>2+</sup> influx in PPZ2-induced prevention of TGF $\beta$ -induced contractile differentiation of RAoSMCs: (a,b) Representative images and quantification of  $\alpha$ -SMA (green) immunofluorescence intensities in TRPC6 (KYD)-expressing RAoSMCs. Scale bars = 50  $\mu$ m. (c,d) Representative images and quantification of SM22 $\alpha$  (green) immunofluorescence intensities in TRPC6 (KYD)-expressing RAoSMCs. Scale bars = 50  $\mu$ m. (e,f) Representative images and quantification of TRPC6 (green) immunofluorescence intensities in TRPC6 (KYD)-expressing RAoSMCs. Scale bars = 30  $\mu$ m. Nuclei were counterstained with DAPI (blue). (g,h) Cell-proliferating activity was assessed by optical density (OD) values in TRPC6 (WT)- and TRPC6 (KYD)-expressing RAoSMCs. Three separate experiments (N = 3) were averaged to produce the data. Data are shown as mean  $\pm$  SEM.  $p < 0.05$  using one-way ANOVA followed by Tukey's post hoc test.

### 3.3. Pharmacological Activation of TRPC6 by PPZ2 Reverses the TGF $\beta$ -Induced Reduction in Intracellular Zn<sup>2+</sup> Amount in RAoSMCs

Next, we investigated the relationship between intracellular Zn<sup>2+</sup> amount and phenotype switching in VSMCs. The released amount of the pooled Zn<sup>2+</sup> evoked by DTDP was significantly reduced in TGF $\beta$ -stimulated TRPC6 (WT)-expressing RAoSMCs, and this reduction was reversed by PPZ2 (Figure 3a,b). The released amount of the pooled Zn<sup>2+</sup> evoked by DTDP was also reduced in TGF $\beta$ -induced TRPC6 (KYD)-expressing RAoSMCs,

but this reduction was never reversed by PPZ2 (Figure 3c,d). These results suggest that PPZ2 contributes to the maintenance of an intracellular pooled  $\text{Zn}^{2+}$  amount in VSMCs through the TRPC6 channel.

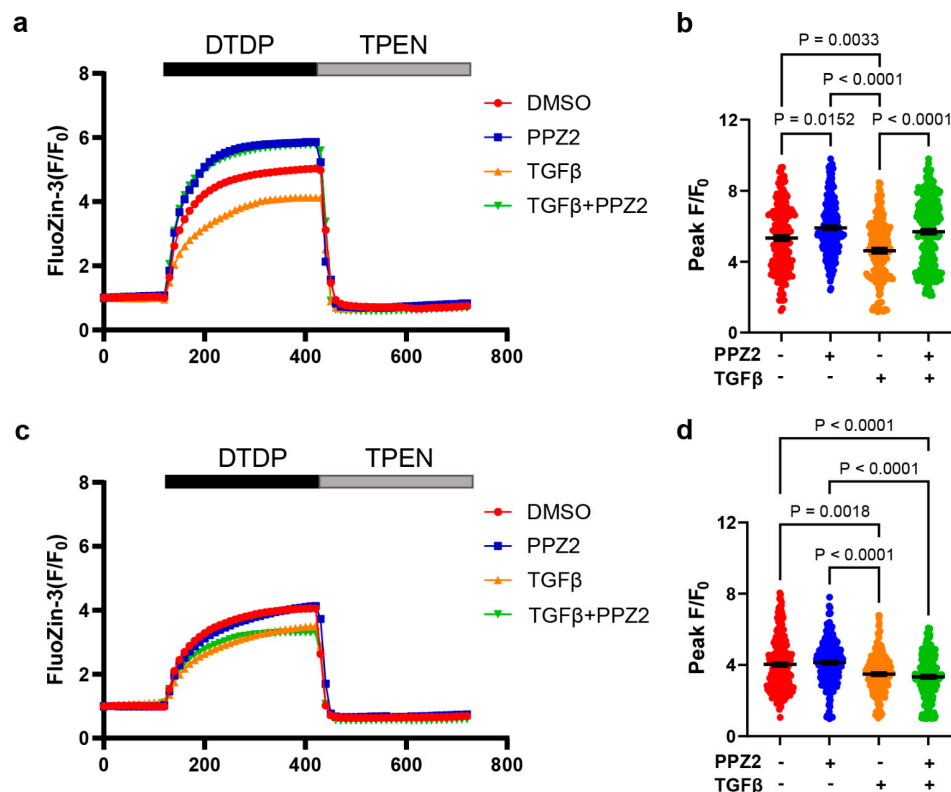


**Figure 3.** Activation of TRPC6-mediated  $\text{Zn}^{2+}$  influx reverses the reduction in intracellular  $\text{Zn}^{2+}$  pool in TGF $\beta$ -stimulated RAoSMCs: **(a,b)** Time courses and peak intensities of FluoZin-3 fluorescence evoked by DTDP in TRPC6 (WT)-expressing RAoSMCs. TPEN chelates intracellular free  $\text{Zn}^{2+}$ . DMSO N = 184 cells; PPZ2 N = 242 cells; TGF $\beta$  N = 189 cells; TGF $\beta$  + PPZ2 N = 267 cells. **(c,d)** Time courses and peak intensities of FluoZin-3 fluorescence evoked by DTDP in TRPC6 (KYD)-expressing RAoSMCs. TPEN chelates intracellular free  $\text{Zn}^{2+}$ . DMSO N = 267 cells; PPZ2 N = 265 cells; TGF $\beta$  N = 245 cells; TGF $\beta$  + PPZ2 N = 245 cells. Experiments were repeated at least 3 times. Data are shown as mean  $\pm$  SEM.  $p < 0.05$  using Kruskal–Wallis test with Dunn test.

#### 3.4. Expression of Functional TRPC6 Protein Levels Are Not Changed in RAoSMCs (WT) and RAoSMCs (KYD) Regardless of Phenotype

We further investigated whether phenotype switching or PPZ2 treatment has some impact on the expression of functional TRPC6 channels in RAoSMCs. TRPC6 channel can permeate cations such as  $\text{Na}^+$ ,  $\text{Ca}^{2+}$  and  $\text{K}^+$ . The total TRPC6-mediated currents detected by whole-cell patch clamp recording were not changed by 24 h PPZ2 or TGF $\beta$  pretreatment in TRPC6 (WT)-expressing RAoSMCs (Figure 4a). No significant differences were observed in TRPC6-mediated current amplitude at  $-90$  mV (Figure 4b). Of note, the electrophysiological properties and currents amplitude of TRPC6 remained unchanged in TRPC6 (KYD)-expressing RAoSMCs, and PPZ2 and/or TGF $\beta$  treatment had no impact on TRPC6-mediated currents at  $-90$  mV (Figure 4c,d). These results clearly suggest that the expression levels of functional TRPC6 channels are not changed among all experiments.

#### 3.5. PPZ2 Attenuates the Ang II-Induced Vascular Remodeling in Mouse Aorta

Ang II enhances the expression or function of TGF $\beta$  receptors on VSMCs to modulate cell growth [46]. We finally examined whether PPZ2 treatment attenuates vascular remodeling caused by Ang II in mice. We confirmed that Ang II-treated mice caused severe hy-



pertension to the same extent in both DMSO- (systolic blood pressure,  $130.1 \pm 1.7$  mmHg) and PPZ2-treated mice (systolic blood pressure,  $129.3 \pm 1.7$  mmHg) (Figure 5a). However, the fluorescence intensities of  $\alpha$ -SMA were increased in the media layer of the arterial vessel wall in chronic Ang II-treated mice, while this increase was canceled by PPZ2 treatment (Figure 5b,c). This result suggests that activation of the TRPC6 channel attenuates pathological vascular remodeling in mice partly through the  $Zn^{2+}$  influx-mediated signaling pathway.

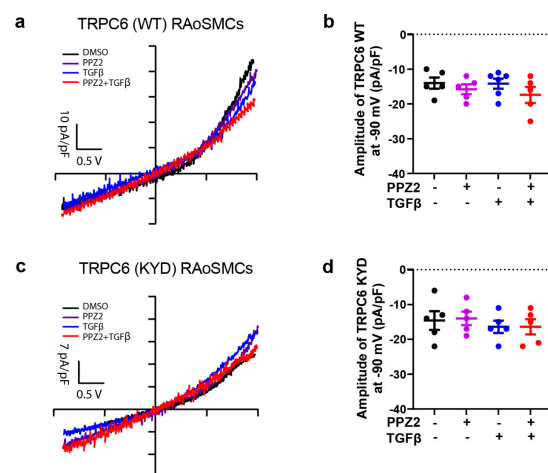


**Figure 4.** Similar electrophysiological properties of TRPC6-mediated currents in TRPC6 (WT)- and TRPC6 (KYD)-expressing RAoSMCs: (a,c) Representative leak-subtracted  $I-V$  relationships of TRPC6 currents recorded in TRPC6 (WT)- and TRPC6 (KYD)-expressing RAoSMCs pretreated with DMSO or PPZ2 (3  $\mu$ M) and with or without TGF $\beta$  (10 ng/mL) for 24 h.  $N = 5$  cells from 3 independent experiments, respectively. (b,d) The amplitude of TRPC6 current at  $-90$  mV. Data are shown as mean  $\pm$  SEM.  $p < 0.05$  using one-way ANOVA followed by Tukey's post hoc test.

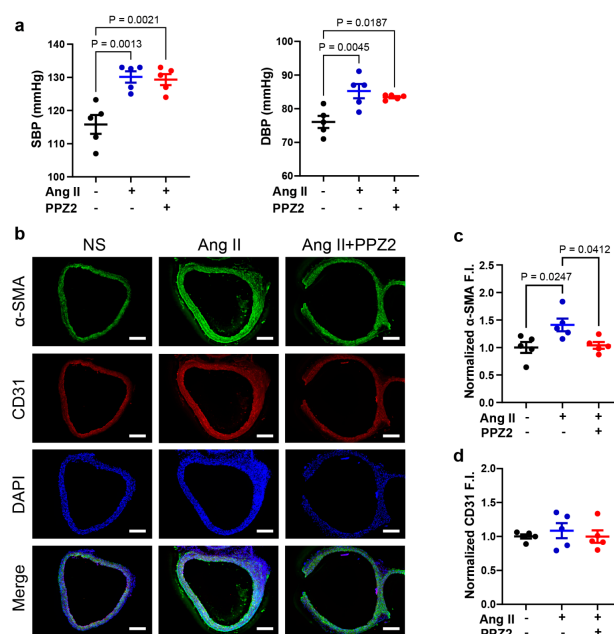


**Figure 5.** PPZ2 attenuates Ang II-induced vascular remodeling in mice aorta: (a) Systolic blood pressure (SBP) and diastolic blood pressure (DBP) in mice. (b) Representative images of  $\alpha$ -SMA (green) and CD31 (red) immunofluorescence staining in mice aortas. (c) Quantification of  $\alpha$ -SMA immunofluorescence intensities. (d) Quantification of CD31 immunofluorescence intensities. Nuclei were counterstained with DAPI (blue). Scale bars = 200  $\mu$ m. Five mice were tested in each group ( $N = 5$ ). Data are shown as mean  $\pm$  SEM.  $p < 0.05$  using one-way ANOVA followed by Tukey's post hoc test.

#### 4. Discussion

Our findings suggest the pivotal role of TRPC6-mediated  $\text{Zn}^{2+}$  influx in regulating VSMCs phenotypic switching, with broader implications in vascular remodeling. Using RAOsMCs (KYD), we successfully separate the role of TRPC6-mediated  $\text{Zn}^{2+}$  influx from TRPC6-mediated other cation influxes and revealed that pharmacological activation of TRPC6 by PPZ2 negatively regulates TGF $\beta$ -induced contractile differentiation of RAOsMCs through  $\text{Zn}^{2+}$  mobilization. Based on this in vitro observation, we also demonstrated using Ang II-treated mice that PPZ2 treatment attenuated pathological vascular remodeling. These findings offer new insights into vascular plasticity and remodeling mechanisms and significant implications for cardiovascular disease management.

Compared to other TRPC channels, the specific  $\text{Zn}^{2+}$  permeability of the TRPC6 channel introduces a new dimension to its regulatory function in cellular homeostasis. Previous studies predominantly focused on TRPC6-mediated  $\text{Ca}^{2+}$  influx in vascular pathologies. TRPC6 deficiency impairs the maintenance of the contractile phenotype in arterial VSMCs, as evidenced by reduced expression of contractile markers, enhanced VSMCs proliferation, and migration, as well as exacerbated neointimal hyperplasia and luminal stenosis in the common carotid arteries (CCA) of TRPC6<sup>(-/-)</sup> mice [47]. We previously reported that activation of the TRPC6 channel by diacylglycerol induces  $\text{Ca}^{2+}$  entry, promoting synthetic switching of VSMCs through membrane depolarization and  $\text{Ca}^{2+}$ -dependent interaction with PTEN [21]. PTEN represses downstream PI3K/Akt signaling, which is necessary for contractile differentiation, by dephosphorylating phosphatidylinositol-3, 4, 5-trisphosphate. In contrast, mobile  $\text{Zn}^{2+}$  is reported to inhibit PTEN, leading to activating the PI3K/Akt pathway of interleukin-2 signaling in T-cells, human airway epithelium, and neurodegeneration [48]. Otherwise,  $\text{Zn}^{2+}$  deficiency reduces the proliferation of transplanted tumors in host animals [49] and decreases the proliferation of rat aorta-origin VSMCs (A7r5 VSMCs) and aortic VSMCs under non-calcifying and calcifying conditions [50]. As the electrophysiological TRPC6 (KYD) channel activity was equivalent to that of TRPC6 (WT) channel activity in RAOsMCs, the mechanism of  $\text{Zn}^{2+}$ -mediated suppression of TGF $\beta$ -induced contractile differentiation must be distinct from  $\text{Ca}^{2+}$ -dependent regulation (Figure 6). Further investigation is required to elucidate how TRPC6-mediated  $\text{Zn}^{2+}$  influx negatively regulates the contractile differentiation, including the underlying signaling pathways.

Our findings highlight  $\text{Zn}^{2+}$  as a critical second messenger in TRPC6-mediated regulation of VSMCs. However, the causal relationship between  $\text{Zn}^{2+}$  dynamics and vascular plasticity has been obscure. Therefore, beyond  $\text{Ca}^{2+}$  signaling, we utilized DTDP to release the intracellular zinc pool to evaluate the interaction of  $\text{Zn}^{2+}$  and phenotype regulation in VSMCs. Our data suggested that pharmacological activation of TRPC6 by PPZ2 alleviated the TGF $\beta$ -induced contractile differentiation and reduction in intracellular  $\text{Zn}^{2+}$  amount in RAOsMCs (WT) but not in RAOsMCs (KYD). These differences suggest that TRPC6-mediated  $\text{Zn}^{2+}$  influx negatively regulates TGF $\beta$ -induced VSMC differentiation through maintaining intracellular  $\text{Zn}^{2+}$  homeostasis.

Vascular injury, characterized by endothelial dysfunction, structural remodeling, inflammation and fibrosis, significantly contributes to the progression of cardiovascular diseases. Cellular processes underlying vascular injury include imbalanced VSMC plasticity, which results in maladaptive phenotypic switching [6]. Ang II signaling pathways become activated with age and contribute to developing arteriosclerosis and vascular senescence. Ang II is one of the numerous factors implicated in vascular injury, it can be converted into smaller, functionally active peptides and play a role in regulating vascular tone and structure [51]. The chronic infusion of Ang II induces the development of several cardiovascular diseases, including cardiac fibrosis [52], atherosclerosis [53] and aortic aneurysms in

mice [54]. Although our Ang II infusion model was insufficient to cause vascular injury, we could observe vascular remodeling after a 4-week Ang II infusion. We demonstrated that activation of the TRPC6 channel by PPZ2 attenuated the Ang II-induced vascular remodeling in mice. Further analyses focusing on TRPC6-mediated  $Zn^{2+}$  influx in vivo should be necessary to establish the therapeutic potential of TRPC6 channel activation against pathological vascular remodeling.

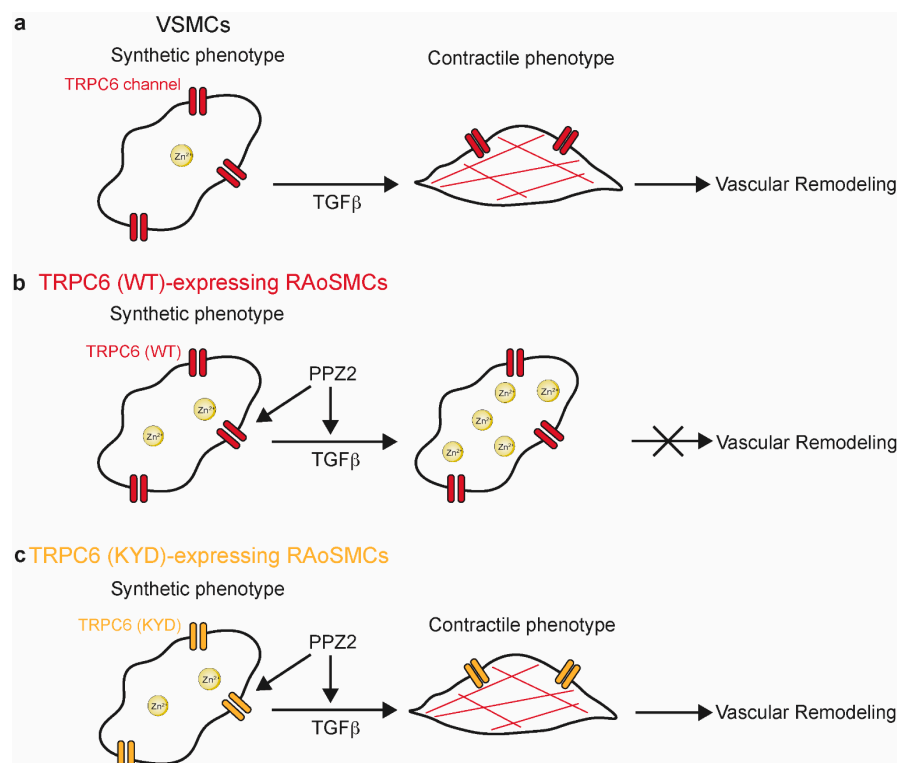


**Figure 6.** Schema of the role of TRPC6-mediated  $Zn^{2+}$  influx in negative regulation of  $TGF\beta$ -induced VSMC contractile differentiation and vascular remodeling: (a) Synthetic phenotype of VSMCs switches into contractile phenotype under  $TGF\beta$  stimulation, which further induced vascular remodeling in vivo. (b,c) Activation of TRPC6 channel by PPZ2 negatively regulates contractile dedifferentiation in TRPC6 (WT)-expressing RAoSMCs (b), which was failed by the specific inhibition of  $Zn^{2+}$  permeability on TRPC6 (c).

## 5. Conclusions

Our findings highlight the pivotal role of TRPC6-mediated  $Zn^{2+}$  influx in modulating VSMC phenotypic plasticity and vascular remodeling, providing novel insights into its potential as a therapeutic target for cardiovascular diseases. These results not only expand the understanding of  $Zn^{2+}$  signaling in vascular biology but also underscore the clinical significance of TRPC6 in regulating vascular function. Future investigations should focus on elucidating the molecular mechanisms underlying TRPC6-mediated  $Zn^{2+}$  signaling, exploring its role across various vascular cell types to fully realize its therapeutic potential.

**Author Contributions:** Conceptualization, M.N.; Methodology, C.S., X.M. and T.I.; Validation, M.N.; Formal Analysis, C.S. and X.M.; Investigation, C.S., X.M., T.I., A.N. and Y.K.; Resources, R.N. and Y.M.; Data Curation, C.S., X.M., T.I., A.N. and Y.K.; Writing—Original Draft Preparation, C.S. and X.M.; Writing—Review and Editing, M.N., X.M., T.I. and C.S.; Visualization, T.I.; Supervision, M.N.; Project Administration, M.N.; Funding Acquisition, T.I. and M.N. All authors have read and agreed to the published version of the manuscript.

**Funding:** This work was supported by JST CREST Grant Number JPMJCR2024 (20348438 to M.N. and A.N.), JSPS KAKENHI (24K23268 to T.I. and 22H02772 to M.N.), Grant-in-Aid for Scientific Research on Innovative Areas (A) “Sulfur biology” (21H05269 and 21H05258 to M.N.) and International Leading Research (23K20040 to M.N.) from the Ministry of Education, Culture, Sports, Science and Technology of Japan, the Naito Foundation (to M.N.) and the Smoking Research Foundation (to M.N.).

**Institutional Review Board Statement:** The animal experiments were reviewed and approved by the Animal Care and Use Committee at Kyushu University and performed according to Institutional Guidelines Concerning the Care and Handling of Experimental Animals (approval no. A24-167-1 and A24-252-1, approval date: 27 August 2024 and 6 August 2024, respectively).

**Informed Consent Statement:** Not applicable.

**Data Availability Statement:** All data generated or analyzed during this study are included in this published article and are available from the corresponding author upon reasonable request.

**Conflicts of Interest:** The authors declare no conflicts of interest.

## References

- Brown, I.A.M.; Diederich, L.; Good, M.E.; DeLalio, L.J.; Murphy, S.A.; Cortese-Krott, M.M.; Hall, J.L.; Le, T.H.; Isakson, B.E. Vascular Smooth Muscle Remodeling in Conductive and Resistance Arteries in Hypertension. *Arterioscler. Thromb. Vasc. Biol.* **2018**, *38*, 1969–1985. [\[CrossRef\]](#) [\[PubMed\]](#)
- Roldán-Montero, R.; Pérez-Sáez, J.M.; Cerro-Pardo, I.; Oller, J.; Martínez-Lopez, D.; Nuñez, E.; Maller, S.M.; Gutierrez-Muñoz, C.; Mendez-Barbero, N.; Escola-Gil, J.C.; et al. Galectin-1 prevents pathological vascular remodeling in atherosclerosis and abdominal aortic aneurysm. *Sci. Adv.* **2022**, *8*, eabm7322. [\[CrossRef\]](#)
- Hoffman, W.E.; Miletich, D.J.; Albrecht, R.F.; Anderson, S. Regional cerebral blood flow measurement in rats with radioactive microspheres. *Life Sci.* **1983**, *33*, 1075–1080. [\[CrossRef\]](#) [\[PubMed\]](#)
- Mazurek, R.; Dave, J.M.; Chandran, R.R.; Misra, A.; Sheikh, A.Q.; Greif, D.M. Vascular Cells in Blood Vessel Wall Development and Disease. *Adv. Pharmacol.* **2017**, *78*, 323–350. [\[CrossRef\]](#) [\[PubMed\]](#)
- Owens, G.K.; Kumar, M.S.; Wamhoff, B.R. Molecular regulation of vascular smooth muscle cell differentiation in development and disease. *Physiol. Rev.* **2004**, *84*, 767–801. [\[CrossRef\]](#) [\[PubMed\]](#)
- Frismantien, A.; Philippova, M.; Erne, P.; Resink, T.J. Smooth muscle cell-driven vascular diseases and molecular mechanisms of VSMC plasticity. *Cell Signal* **2018**, *52*, 48–64. [\[CrossRef\]](#)
- Zhang, C.Y.; Hu, Y.C.; Zhang, Y.; Ma, W.D.; Song, Y.F.; Quan, X.H.; Guo, X.; Wang, C.X. Glutamine switches vascular smooth muscle cells to synthetic phenotype through inhibiting miR-143 expression and upregulating THY1 expression. *Life Sci.* **2021**, *277*, 119365. [\[CrossRef\]](#) [\[PubMed\]](#)
- Tang, H.Y.; Chen, A.Q.; Zhang, H.; Gao, X.F.; Kong, X.Q.; Zhang, J.J. Vascular Smooth Muscle Cells Phenotypic Switching in Cardiovascular Diseases. *Cells* **2022**, *11*, 4060. [\[CrossRef\]](#) [\[PubMed\]](#)
- Bennett, M.R.; Sinha, S.; Owens, G.K. Vascular Smooth Muscle Cells in Atherosclerosis. *Circ. Res.* **2016**, *118*, 692–702. [\[CrossRef\]](#) [\[PubMed\]](#)
- Davis-Dusenbery, B.N.; Wu, C.; Hata, A. Micromanaging vascular smooth muscle cell differentiation and phenotypic modulation. *Arterioscler. Thromb. Vasc. Biol.* **2011**, *31*, 2370–2377. [\[CrossRef\]](#)
- Ip, J.H.; Fuster, V.; Badimon, L.; Badimon, J.; Taubman, M.B.; Chesebro, J.H. Syndromes of accelerated atherosclerosis: Role of vascular injury and smooth muscle cell proliferation. *J. Am. Coll. Cardiol.* **1990**, *15*, 1667–1687. [\[CrossRef\]](#)
- Kocher, O.; Gabbiani, G. Cytoskeletal features of normal and atheromatous human arterial smooth muscle cells. *Hum. Pathol.* **1986**, *17*, 875–880. [\[CrossRef\]](#)
- Libby, P. Current concepts of the pathogenesis of the acute coronary syndromes. *Circulation* **2001**, *104*, 365–372. [\[CrossRef\]](#) [\[PubMed\]](#)
- Miano, J.M.; Cserjesi, P.; Ligon, K.L.; Periasamy, M.; Olson, E.N. Smooth muscle myosin heavy chain exclusively marks the smooth muscle lineage during mouse embryogenesis. *Circ. Res.* **1994**, *75*, 803–812. [\[CrossRef\]](#) [\[PubMed\]](#)
- Nishimura, A.; Sunggip, C.; Tozaki-Saitoh, H.; Shimauchi, T.; Numaga-Tomita, T.; Hirano, K.; Ide, T.; Boeynaems, J.M.; Kurose, H.; Tsuda, M.; et al. Purinergic P2Y6 receptors heterodimerize with angiotensin AT1 receptors to promote angiotensin II-induced hypertension. *Sci. Signal* **2016**, *9*, ra7. [\[CrossRef\]](#)
- Hofmann, T.; Obukhov, A.G.; Schaefer, M.; Harteneck, C.; Gudermann, T.; Schultz, G. Direct activation of human TRPC6 and TRPC3 channels by diacylglycerol. *Nature* **1999**, *397*, 259–263. [\[CrossRef\]](#) [\[PubMed\]](#)

17. Nishida, M.; Tanaka, T.; Mangmool, S.; Nishiyama, K.; Nishimura, A. Canonical Transient Receptor Potential Channels and Vascular Smooth Muscle Cell Plasticity. *J. Lipid Atheroscler.* **2020**, *9*, 124–139. [[CrossRef](#)] [[PubMed](#)]
18. Fernandez, R.A.; Wan, J.; Song, S.; Smith, K.A.; Gu, Y.; Tauseef, M.; Tang, H.; Makino, A.; Mehta, D.; Yuan, J.X. Upregulated expression of STIM2, TRPC6, and Orai2 contributes to the transition of pulmonary arterial smooth muscle cells from a contractile to proliferative phenotype. *Am. J. Physiol. Cell Physiol.* **2015**, *308*, C581–C593. [[CrossRef](#)]
19. Golovina, V.A.; Platoshyn, O.; Bailey, C.L.; Wang, J.; Limsuwan, A.; Sweeney, M.; Rubin, L.J.; Yuan, J.X. Upregulated TRP and enhanced capacitative Ca(2+) entry in human pulmonary artery myocytes during proliferation. *Am. J. Physiol. Heart Circ. Physiol.* **2001**, *280*, H746–H755. [[CrossRef](#)] [[PubMed](#)]
20. Numaga-Tomita, T.; Shimauchi, T.; Kato, Y.; Nishiyama, K.; Nishimura, A.; Sakata, K.; Inada, H.; Kita, S.; Iwamoto, T.; Nabekura, J.; et al. Inhibition of transient receptor potential cation channel 6 promotes capillary arterIALIZATION during post-ischaemic blood flow recovery. *Br. J. Pharmacol.* **2023**, *180*, 94–110. [[CrossRef](#)]
21. Numaga-Tomita, T.; Shimauchi, T.; Oda, S.; Tanaka, T.; Nishiyama, K.; Nishimura, A.; Birnbaumer, L.; Mori, Y.; Nishida, M. TRPC6 regulates phenotypic switching of vascular smooth muscle cells through plasma membrane potential-dependent coupling with PTEN. *FASEB J.* **2019**, *33*, 9785–9796. [[CrossRef](#)] [[PubMed](#)]
22. Chevallet, M.; Jarvis, L.; Harel, A.; Luche, S.; Degot, S.; Chapuis, V.; Boulay, G.; Rabilloud, T.; Bouron, A. Functional consequences of the over-expression of TRPC6 channels in HEK cells: Impact on the homeostasis of zinc. *Metallomics* **2014**, *6*, 1269–1276. [[CrossRef](#)]
23. Gibon, J.; Tu, P.; Bohic, S.; Richaud, P.; Arnaud, J.; Zhu, M.; Boulay, G.; Bouron, A. The over-expression of TRPC6 channels in HEK-293 cells favours the intracellular accumulation of zinc. *Biochim. Biophys. Acta* **2011**, *1808*, 2807–2818. [[CrossRef](#)] [[PubMed](#)]
24. Hasna, J.; Abi Nahed, R.; Sergeant, F.; Alfaidy, N.; Bouron, A. The Deletion of TRPC6 Channels Perturbs Iron and Zinc Homeostasis and Pregnancy Outcome in Mice. *Cell Physiol. Biochem.* **2019**, *52*, 455–467. [[CrossRef](#)]
25. Oda, S.; Nishiyama, K.; Furumoto, Y.; Yamaguchi, Y.; Nishimura, A.; Tang, X.; Kato, Y.; Numaga-Tomita, T.; Kaneko, T.; Mangmool, S.; et al. Myocardial TRPC6-mediated Zn(2+) influx induces beneficial positive inotropy through  $\beta$ -adrenoceptors. *Nat. Commun.* **2022**, *13*, 6374. [[CrossRef](#)]
26. Trebak, M.; Vazquez, G.; Bird, G.S.; Putney, J.W., Jr. The TRPC3/6/7 subfamily of cation channels. *Cell Calcium* **2003**, *33*, 451–461. [[CrossRef](#)]
27. Maret, W. Zinc in Cellular Regulation: The Nature and Significance of “Zinc Signals”. *Int. J. Mol. Sci.* **2017**, *18*, 2285. [[CrossRef](#)]
28. Takeda, A.; Tamano, H. Insight into brain metallothioneins from bidirectional Zn<sup>2+</sup> signaling in synaptic dynamics. *Metallomics* **2024**, *16*, mfae039. [[CrossRef](#)]
29. Yamasaki, S.; Sakata-Sogawa, K.; Hasegawa, A.; Suzuki, T.; Kabu, K.; Sato, E.; Kurosaki, T.; Yamashita, S.; Tokunaga, M.; Nishida, K.; et al. Zinc is a novel intracellular second messenger. *J. Cell Biol.* **2007**, *177*, 637–645. [[CrossRef](#)] [[PubMed](#)]
30. Zhang, M.; Ma, Y.; Ye, X.; Zhang, N.; Pan, L.; Wang, B. TRP (transient receptor potential) ion channel family: Structures, biological functions and therapeutic interventions for diseases. *Signal Transduct. Target. Ther.* **2023**, *8*, 261. [[CrossRef](#)] [[PubMed](#)]
31. Inoue, K.; O'Bryant, Z.; Xiong, Z.G. Zinc-permeable ion channels: Effects on intracellular zinc dynamics and potential physiological/pathophysiological significance. *Curr. Med. Chem.* **2015**, *22*, 1248–1257. [[CrossRef](#)]
32. Aizenman, E.; Stout, A.K.; Hartnett, K.A.; Dineley, K.E.; McLaughlin, B.; Reynolds, I.J. Induction of neuronal apoptosis by thiol oxidation: Putative role of intracellular zinc release. *J. Neurochem.* **2000**, *75*, 1878–1888. [[CrossRef](#)]
33. Anson, K.J.; Corbet, G.A.; Palmer, A.E. Zn(2+) influx activates ERK and Akt signaling pathways. *Proc. Natl. Acad. Sci. USA* **2021**, *118*, e2015786118. [[CrossRef](#)] [[PubMed](#)]
34. MacDonald, R.S. The role of zinc in growth and cell proliferation. *J. Nutr.* **2000**, *130*, 1500s–1508s. [[CrossRef](#)]
35. Li, Y.; Maret, W. Transient fluctuations of intracellular zinc ions in cell proliferation. *Exp. Cell Res.* **2009**, *315*, 2463–2470. [[CrossRef](#)]
36. Sawamura, S.; Hatano, M.; Takada, Y.; Hino, K.; Kawamura, T.; Tanikawa, J.; Nakagawa, H.; Hase, H.; Nakao, A.; Hirano, M.; et al. Screening of Transient Receptor Potential Canonical Channel Activators Identifies Novel Neurotrophic Piperazine Compounds. *Mol. Pharmacol.* **2016**, *89*, 348–363. [[CrossRef](#)] [[PubMed](#)]
37. Shimauchi, T.; Numaga-Tomita, T.; Kato, Y.; Morimoto, H.; Sakata, K.; Matsukane, R.; Nishimura, A.; Nishiyama, K.; Shibuta, A.; Horiuchi, Y.; et al. A TRPC3/6 Channel Inhibitor Promotes Arteriogenesis after Hind-Limb Ischemia. *Cells* **2022**, *11*, 2041. [[CrossRef](#)]
38. Kojima, A.; Kitagawa, H.; Omatsu-Kanbe, M.; Matsuura, H.; Nosaka, S. Ca<sup>2+</sup> paradox injury mediated through TRPC channels in mouse ventricular myocytes. *Br. J. Pharmacol.* **2010**, *161*, 1734–1750. [[CrossRef](#)] [[PubMed](#)]
39. Mishra, P.; Pandey, C.M.; Singh, U.; Gupta, A.; Sahu, C.; Keshri, A. Descriptive statistics and normality tests for statistical data. *Ann. Card. Anaesth.* **2019**, *22*, 67–72. [[CrossRef](#)] [[PubMed](#)]
40. Hirschi, K.K.; Rohovsky, S.A.; D'Amore, P.A. PDGF, TGF-beta, and heterotypic cell-cell interactions mediate endothelial cell-induced recruitment of 10T1/2 cells and their differentiation to a smooth muscle fate. *J. Cell Biol.* **1998**, *141*, 805–814. [[CrossRef](#)]



41. Johansson-Percival, A.; Li, Z.J.; Lakhiani, D.D.; He, B.; Wang, X.; Hamzah, J.; Ganss, R. Intratumoral LIGHT Restores Pericyte Contractile Properties and Vessel Integrity. *Cell Rep.* **2015**, *13*, 2687–2698. [[CrossRef](#)] [[PubMed](#)]
42. Li, F.; Luo, Z.; Huang, W.; Lu, Q.; Wilcox, C.S.; Jose, P.A.; Chen, S. Response gene to complement 32, a novel regulator for transforming growth factor-beta-induced smooth muscle differentiation of neural crest cells. *J. Biol. Chem.* **2007**, *282*, 10133–10137. [[CrossRef](#)] [[PubMed](#)]
43. Mainland, D. Statistical ward round. 16. *Clin. Pharmacol. Ther.* **1969**, *10*, 576–586. [[CrossRef](#)] [[PubMed](#)]
44. Shi, N.; Xie, W.B.; Chen, S.Y. Cell division cycle 7 is a novel regulator of transforming growth factor- $\beta$ -induced smooth muscle cell differentiation. *J. Biol. Chem.* **2012**, *287*, 6860–6867. [[CrossRef](#)] [[PubMed](#)]
45. Soboloff, J.; Spassova, M.; Xu, W.; He, L.P.; Cuesta, N.; Gill, D.L. Role of endogenous TRPC6 channels in  $\text{Ca}^{2+}$  signal generation in A7r5 smooth muscle cells. *J. Biol. Chem.* **2005**, *280*, 39786–39794. [[CrossRef](#)] [[PubMed](#)]
46. Fukuda, N.; Hu, W.Y.; Kubo, A.; Kishioka, H.; Satoh, C.; Soma, M.; Izumi, Y.; Kanmatsuse, K. Angiotensin II upregulates transforming growth factor-beta type I receptor on rat vascular smooth muscle cells. *Am. J. Hypertens.* **2000**, *13*, 191–198. [[CrossRef](#)] [[PubMed](#)]
47. Smith, A.H.; Putta, P.; Driscoll, E.C.; Chaudhuri, P.; Birnbaumer, L.; Rosenbaum, M.A.; Graham, L.M. Canonical transient receptor potential 6 channel deficiency promotes smooth muscle cells dedifferentiation and increased proliferation after arterial injury. *JVS Vasc. Sci.* **2020**, *1*, 136–150. [[CrossRef](#)]
48. Plum, L.M.; Brieger, A.; Engelhardt, G.; Hebel, S.; Nessel, A.; Arlt, M.; Kaltenberg, J.; Schwaneberg, U.; Huber, M.; Rink, L.; et al. PTEN-inhibition by zinc ions augments interleukin-2-mediated Akt phosphorylation. *Metallomics* **2014**, *6*, 1277–1287. [[CrossRef](#)] [[PubMed](#)]
49. DeWys, W.; Pories, W. Inhibition of a spectrum of animal tumors by dietary zinc deficiency. *J. Natl. Cancer Inst.* **1972**, *48*, 375–381.
50. Alcantara, E.H.; Shin, M.Y.; Feldmann, J.; Nixon, G.F.; Beattie, J.H.; Kwun, I.S. Long-term zinc deprivation accelerates rat vascular smooth muscle cell proliferation involving the down-regulation of JNK1/2 expression in MAPK signaling. *Atherosclerosis* **2013**, *228*, 46–52. [[CrossRef](#)]
51. Montezano, A.C.; Nguyen Dinh Cat, A.; Rios, F.J.; Touyz, R.M. Angiotensin II and vascular injury. *Curr. Hypertens. Rep.* **2014**, *16*, 431. [[CrossRef](#)]
52. Yu, Y.H.; Zhang, Y.H.; Ding, Y.Q.; Bi, X.Y.; Yuan, J.; Zhou, H.; Wang, P.X.; Zhang, L.L.; Ye, J.T. MicroRNA-99b-3p promotes angiotensin II-induced cardiac fibrosis in mice by targeting GSK-3 $\beta$ . *Acta Pharmacol. Sin.* **2021**, *42*, 715–725. [[CrossRef](#)] [[PubMed](#)]
53. Kunieda, T.; Minamino, T.; Nishi, J.; Tateno, K.; Oyama, T.; Katsuno, T.; Miyauchi, H.; Orimo, M.; Okada, S.; Takamura, M.; et al. Angiotensin II induces premature senescence of vascular smooth muscle cells and accelerates the development of atherosclerosis via a p21-dependent pathway. *Circulation* **2006**, *114*, 953–960. [[CrossRef](#)]
54. Lu, H.; Howatt, D.A.; Balakrishnan, A.; Moorleggen, J.J.; Rateri, D.L.; Cassis, L.A.; Daugherty, A. Subcutaneous Angiotensin II Infusion using Osmotic Pumps Induces Aortic Aneurysms in Mice. *J. Vis. Exp.* **2015**, 53191. [[CrossRef](#)]

**Disclaimer/Publisher’s Note:** The statements, opinions and data contained in all publications are solely those of the individual author(s) and contributor(s) and not of MDPI and/or the editor(s). MDPI and/or the editor(s) disclaim responsibility for any injury to people or property resulting from any ideas, methods, instructions or products referred to in the content.